Research Report

Friction Characteristics Analysis for Clamping Force Setup in Metal V-belt Type CVTs

Hiroyuki Nishizawa, Hiroyuki Yamaguchi, Hideyuki Suzuki

金属ベルト式ＣＶＴにおける挟圧力設定のための摩擦特性解析

西澤博幸，山口裕之，鈴木秀之

Abstract

Lowering the belt clamping force from the current setting value is effective for increasing the transfer efficiency in a metal V-belt type CVT (Continuously Variable Transmission). However, setting the clamping force too low will cause macro slip (large belt slip). Setting of the clamping force to the proper level therefore requires a detailed understanding of the friction characteristics between the belt and the pulley (belt friction characteristics) and requires that the macro slip threshold be clearly defined. In this paper, we propose a friction expression model for a metal V-belt type CVT and use this model to clarify the state of power transmission in the vicinity of the macro slip limit.

Keywords Continuously variable transmission (CVT), Belt, Friction coefficient, Friction expression model, Transfer efficiency

要　旨

金属ベルト式CVT (Continuously Variable Transmission) の伝達効率を向上させるためには，ベルト挟圧力を現状設定値より下げることが有効であるが，下げすぎるとマクロスリップ (大きなベルト滑り) を起こす。このため，適正な挟圧力を設定するためには，ベルトとプーリ間の摩擦特性 (ベルト摩擦特性) を詳細に把握し，マクロスリップ限界を明確にする必要がある。そこで本論文では，金属ベルト式CVTの摩擦発現モデルを提案し，これを用いて，マクロスリップ限界付近での動力伝達状態を明らかにする。

キーワード 無段変速機 (CVT)，ベルト，摩擦係数，摩擦発現モデル，伝達効率

1. Introduction

Recently, the number of vehicles incorporating metal V-belt type CVTs, which can follow the engine optimal fuel consumption curve, have increased to meet CO_2 emissions regulations. However, a problem with current CVTs is that the transmission efficiency is lower than that of conventional automatic transmissions[1] because the current CVTs have large pump drive torque and friction losses in the belt. Transmission efficiency must therefore be improved. An effective means for doing this is to increase the transfer efficiency in CVTs by setting the clamping force in a range sufficiently low that macro slip does not occur (**Fig. 1**). In the figure, the transmission torque capacity of the CVT is proportional to the product of the belt friction coefficient and the clamping force. Accordingly, the transmission efficiency can be maximized by setting the clamping force as follows. First, after the state of the power transmission and the friction characteristics of the belt are clarified, the basic clamping force (clamping force at the macro slip limit) can be set from the maximum friction coefficient and the transmission torque. Next, the margin clamping force corresponding to the disturbance torque that enters from the tires due to factors such a poor roads is added to the basic clamping force.

Existing research on the transfer characteristics of belts includes a paper by Kobayashi,[2] which examines the transfer torque limit using a method that corrects the belt slip model with the friction coefficient characteristic of the individual elements. The paper, however, makes no reference to the belt friction characteristics.

In this paper, we propose a belt friction expression model to explain the belt friction phenomena from the micro slip area to the macro slip area. Using this model, we clarify the state of power transmission in the vicinity of the macro slip limit.

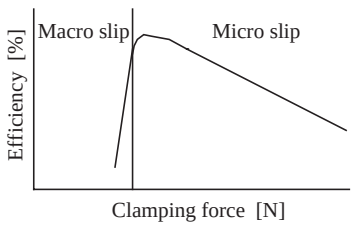

Fig. 1 Clamping force and transfer efficiency.

2. Definition of the belt friction coefficient

When frictional torque is transmitted, the relation between the belt friction coefficient μ and the transmission torque T is shown by Eq. (1) by using the normal force F and the radius R (**Fig. 2**(a)).

$$T = \mu \cdot F \cdot R \quad \cdots\cdots\cdots\cdots\cdots\cdots (1)$$

In this paper, the belt friction coefficient is defined by Eqs. (2) and (3), which correct the pulley surface cone angle θ and the number of friction sides. The need for these corrections is due to a problem caused by the friction between the pulley and the belt (Fig. 2(b)). The belt friction coefficient is defined by Eq. (2), which is defined for the input pulley (primary pulley) when the speed reducing ratio is the decelerating side (speed reducing ratio $\gamma > 1$), since macro slip occurs on the pulley with a small pitch radius. When the speed reducing ratio is the accelerating side ($\gamma < 1$), the belt friction coefficient is defined by Eq. (3), which is defined for the output pulley (secondary pulley). At a constant speed ($\gamma = 1$) in a driving state, since the primary side clamping force Fp is larger than the secondary side clamping force Fs, macro slip occurs on the secondary side, and therefore Eq. (3) is used.

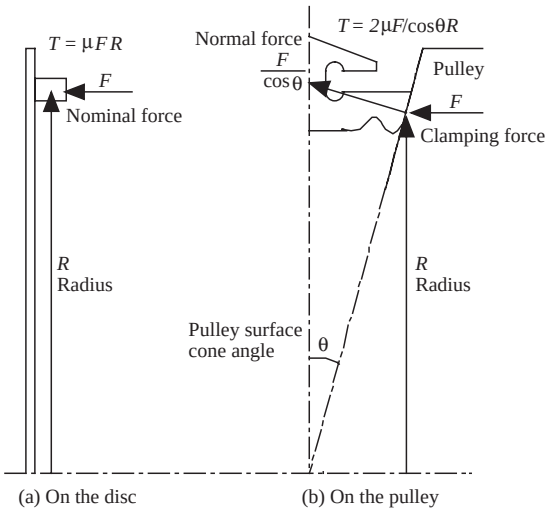

Fig. 2 Force acting.

$$\mu p = T_{in} \cdot \cos\theta / (2 \cdot Fp \cdot Rp) \quad \cdots\cdots\cdots (2)$$

$$\mu s = T_{out} \cdot \cos\theta / (2 \cdot Fs \cdot Rs) \quad \cdots\cdots\cdots (3)$$

μp: Belt friction coefficient for the primary side

T_{in}: Input axis torque (Nm)

Fp: Clamping force for the primary side (N)

Rp: Pitch radius of the pulley for the primary side (m)

θ : Pulley surface cone angle (rad)

μs : belt friction coefficient for the secondary side

T_{out}: Output axis torque (Nm)

Fs: Clamping force for the secondary side (N)

Rs: Pitch radius of the pulley for the secondary side (m)

Also, the belt slip speed Δv is calculated separately for the primary side and the secondary side with Eqs. (4) and (5) to examine the belt friction μ–v characteristics.

$$\Delta v = \Delta vp = Rp \cdot \omega p - v \quad \cdots\cdots\cdots\cdots (4)$$

$$\Delta v = \Delta vs = v - Rs \cdot \omega s \quad \cdots\cdots\cdots\cdots (5)$$

Δvp: Belt slip speed for the primary side (m/s)

ωp: Rotation speed of the primary pulley (rad/s)

v: Belt speed (m/s)

Δvs: Belt slip speed for the secondary side (m/s)

ωs: Rotation speed of the secondary pulley (rad/s)

3. Belt friction characteristics

3. 1 Belt friction expression model

We propose the following belt friction expression mode[13] to describe the belt friction characteristics from the micro slip area to the macro slip area.

We examine the belt friction coefficient μ defined in Eqs. (2) and (3).

The belt friction coefficient μ has different characteristics from the friction coefficient defined for normal intermetallic friction. The belt slip speed and the belt friction coefficient increase when the transmission torque increases. When the belt friction coefficient assumes the maximum value (μ_{max}), the belt friction coefficient decreases according to the increase in belt slip speed (**Fig. 3**). In Fig. 3, the friction coefficient of each of the elements that make up the belt is equal to the friction coefficient defined by intermetallic friction. If this value is then multiplied by the pitch radius and the clamping force, the result is the amount of torque transmittable by one of the elements. The transfer torque of the belt is equivalent to the potential transfer torque of one of the elements multiplied by the number of elements that are actually at work. The region where these elements are actually at work is called the active arc. Because the compression force in the direction of movement of the element changes within the active arc, a transfer force occurs between the pulley and belt (**Fig. 4**). Based on the above, the belt friction coefficient μ as defined by the relationship between the clamping force and the transfer torque can be expressed as the element coefficient μe multiplied by the active arc ratio β/α, as shown in Eq. (6). The active arc ratio β/α is equal to the ratio of the number of elements that actually work and the total number of elements within the pulley. Force transfer in a belt type CVT includes force that is transmitted from more than just the active arc through the metal band bundling the elements. However, these are ignored as their impact is negligible if the active arc ratio β/α is close to 1.

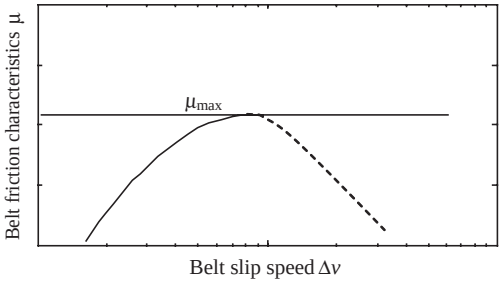

Fig. 3 Belt friction characteristics.

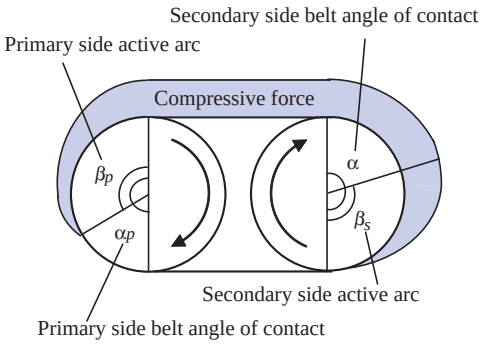

Fig. 4 Active arc in metal v-belt type CVT.

$$\mu = \mu e \cdot \beta/\alpha \quad \cdots\cdots\cdots\cdots\cdots\cdots (6)$$

α: Belt angle of contact (rad)
(The internal pulley angle at which the pulley is fitted around the elements)
β: Active arc (rad)

From Eq. (6), all elements in the pulley begin to slip uniformly and enter an all-slip state when the active arc ratio β/α becomes 1. At this point, the belt friction characteristics and the element friction characteristics coincide (**Fig. 5**).

As the transfer torque increases, the active arc β expands as explained above. However, as shown in Eq. (7), there is a relationship between the active arc β and the belt slip rate.[2] Equation (7) is derived from the idea that the total belt gap δt collects in the idle arc $(\alpha-\beta)$, and the ratio of the idle arc length $(\alpha-\beta)\cdot R + Le$ and the total gap δt becomes the belt slip rate.

$$\text{Slip rate} = \delta t /((\alpha-\beta)\cdot R + Le) \quad \cdots\cdots\cdots (7)$$

δt: Total gap (the total of the gaps between the elements) (m)
R: Pitch radius of the pulley (m)
Le: Element thickness (m)

Accordingly, the belt slip speed Δv is derived by multiplying Eq. (7) by the pulley tangential speed $R\cdot\omega$.

$$\Delta vp = \delta tp / ((\alpha p-\beta p)\cdot Rp+Le)\cdot Rp\cdot\omega p \quad \cdots\cdot (8)$$

$$\Delta vs = \delta ts / ((\alpha s-\beta s)\cdot Rs+Le)\cdot Rs\cdot\omega s \quad \cdots\cdot (9)$$

In these equations, the subscripts p and s refer to the primary side and secondary side, respectively. Also, the total gap δt is postulated as follows. On the primary side, the belt gap in the original position and the gap increased by the tension arising from the clamping force are dominant. Within a narrow range around the maximum transfer torque, the total gap δtp is almost a constant value. Meanwhile, on the secondary side, the elements enter the pulley in a state of compression and this compressive force will only be released when the elements exit the pulley (Fig. 4), so belt slippage occurs for only the amount of elastic deformation. As a result, the entire gap δts (the summation of the amount of elastic deformation on the secondary side) is thought to be almost completely proportional to the transfer torque T_{out}. However, to keep matters simple, we assumed that it is proportional to the active arc ratio $\beta s/\alpha s$ on the secondary side.

$$\delta tp = \text{const.} \quad \cdots\cdots\cdots\cdots\cdots (10)$$

$$\delta ts = \kappa\cdot \beta s/\alpha s \quad \cdots\cdots\cdots\cdots\cdots (11)$$

κ: Proportional coefficient

By employing Eqs. (8) - (11), the relationship between the belt friction coefficient μ and the belt slip speed Δv can be shown.

3. 2 Validity test of the belt friction expression model

For this paper, a CVU (Continuously Variable Unit) test device in which the speed reducing ratio was controlled by hydraulics (**Fig. 6**) was used to measure friction characteristics according to, as much possible, the actual operating conditions of belt type CVTs. The CVU shown in the figure consists of pulleys and a belt. The hydraulic pressure for speed reducing ratio control is supplied by an external hydraulic power unit and uses a servo valve to control the speed reducing ratio on the primary side and the clamping force on the secondary side. The measuring system requires the setting up of a torque meter on the input/output axis and use of the

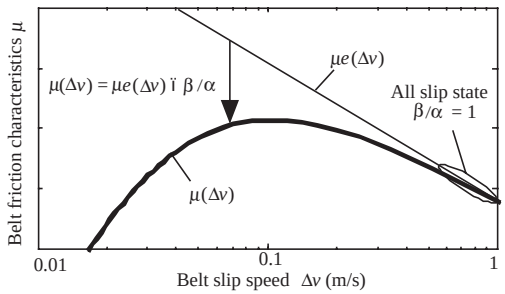

Fig. 5 Proposed belt friction model.

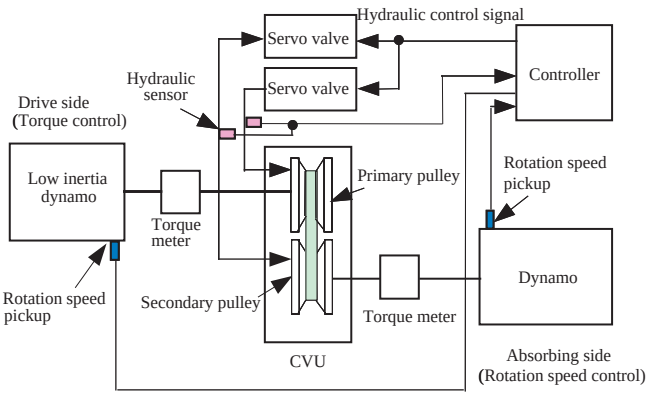

Fig. 6 Schematic of test rig.

dynamo rotation speed to measure the pulley rotation speed. The primary and secondary hydraulic pressures are measured using hydraulic pressure sensors. The primary and secondary clamping forces are calculated by correcting each of the centrifugal oil pressures. The pitch radius of the pulley and the belt speed were measured by attaching the device shown in **Fig. 7**(a) to the CVU. The pitch radius of the pulley was measured using a linear gauge to whose tip was attached a hard alloy chip. The gauge was pressed against the tip of the belt and was attached and positioned as shown in Fig. 7(b).

Figure 8 shows the experimental result when we set the speed reducing ratio γ to 0.65 and kept the secondary side clamping force constant while slowly increasing the input torque to cause a macro slip. The belt friction coefficient μ in the figure is based on Eq. (3). In the driving state (T_{in}>0), because macro slip occurs on the secondary side when γ = 0.65, the friction coefficient and slip speed are shown along with the secondary side data. However, we normalized the friction coefficient by dividing it by the maximum friction coefficient obtained in this experiment μ_{max}(γ = 0.65). The normalized friction coefficients μ^* are defined by Eq. (12).

$$\mu^* = \mu / \mu_{max} \ (\gamma = 0.65) \quad \cdots\cdots\cdots\cdots\cdots (12)$$

Figure 8 also shows the block-on-ring test results. In the negative slope region (Δv > 0.3m/s) of the belt friction characteristics in Fig. 8, all of the elements fitted around the pulley are in a state of uniform slippage and the belt friction characteristics in this region coincide with the element friction characteristics. The reason that the absolute values of the block-on-ring test results and the belt friction characteristics in the all-slip state do not coincide is due to the fact that the state of the contact surface of the elements is different for the ring and for the pulley.

The relation of the belt friction coefficient μ and the active arc ratio β/α calculated by the proposed belt friction expression model is shown in **Fig. 9**. In the figure, the total gap δts is given by assuming the amount of the elasticity deformation of the belt (torque capacity 200 Nm) for speed reducing ratio γ = 0.65. The belt friction coefficient μ increases when the active arc ratio β/α increases. However, the belt friction coefficient μ takes the maximum value (μ_{max}) before the active arc ratio β/α becomes 1. Thereafter, the belt friction coefficient μ decreases as the belt slip speed increases. This relation changes to the relation between the belt slip speed and the belt friction coefficient, which is compared with the experimental data in **Fig. 10**. Figure 10 shows that the calculated result of the model and the experimental result correlate well.

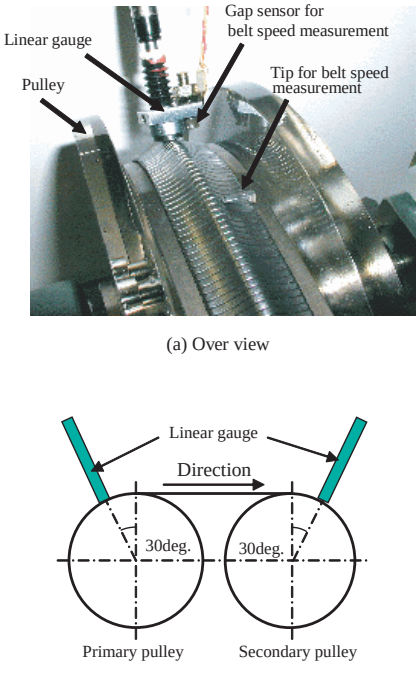

(a) Over view

(b) Installation position relation of linear gauges

Fig. 7 Measurement equipment of the pitch radius of the pulley and the belt speed.

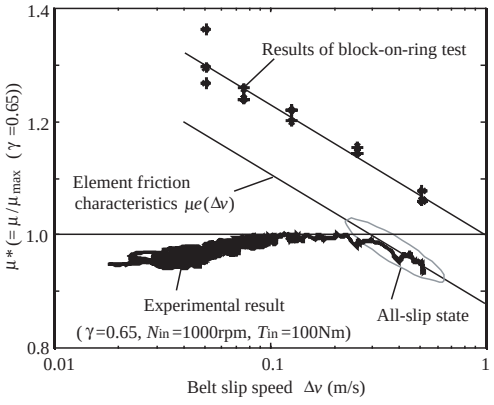

Fig. 8 Belt friction characteristics (γ = 0.65).

Similarly, the belt friction characteristics when the speed reducing ratio changes to γ = 1.5, 2.3 are shown in **Fig. 11**. The total gap δtp was measured by using a fixed speed reducing ratio pulley test rig whose axial tension was set for the belt friction expression model. The calculated result of the model reproduces the speed reducing ratio dependency of the belt friction coefficient well, even though the speed reducing ratio is changed.

3. 3 Consideration of the macro slip limit

It has been thought that the belt friction coefficient achieves the maximum value when all elements in the pulley transmit the power and the belt slip state that exceeds the maximum friction coefficient (μ_{max}) is the all-slip state. However, it is also thought that the elements that do not transmit power remain at the maximum friction coefficient point because the active arc ratio β/α is less than 1 (Fig. 9). This is the point from which the state of power transmission from the micro slip state to the macro slip state is considered.

In the small belt slip region (light load region), power is transmitted in a state in which active arc β is narrow and idle arc α–β is wide (shown in Fig. 12). Therefore, the belt friction coefficient increases as the number of elements that transmit power increases when the transmission torque also increases. However, the increase in belt slip speed is gradual because the idle arc α–β is still wide (see Eqs. (8) and (9)).

When the transmission torque limit is reached, power is transmitted in a state in which active arc β is wide and idle arc α–β is narrow. Therefore, the belt slip speed increases rapidly when the number of elements that transmit power increases while idle arc α–β decreases.

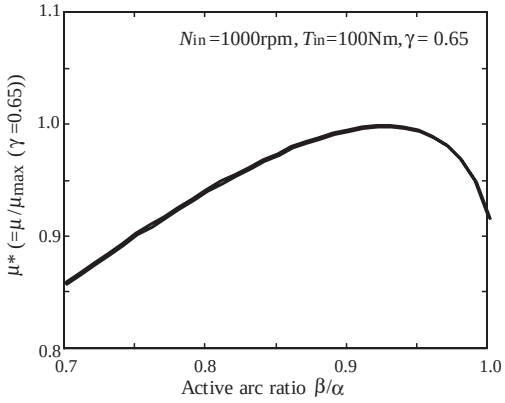

Fig. 9 Relation between belt friction coefficient and active arc ratio in the belt friction expression model.

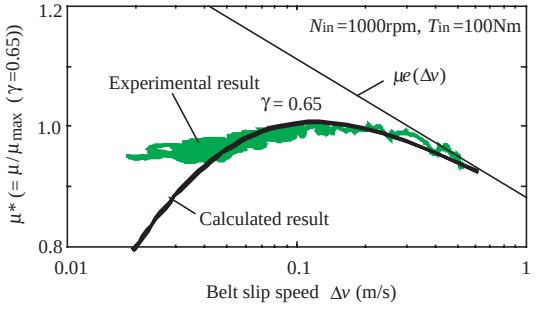

Fig. 10 Comparison between experimental result and calculated result (γ = 0.65).

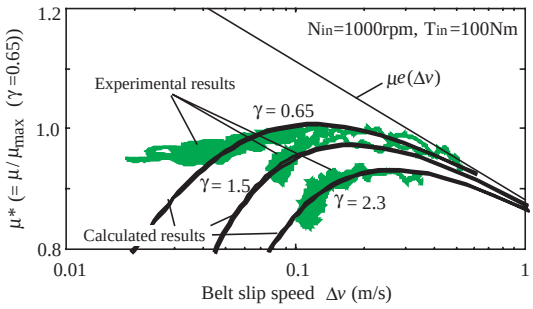

Fig. 11 Difference in the friction characteristics by speed reducing ratio (γ = 0.65, 1.5, 2.3).

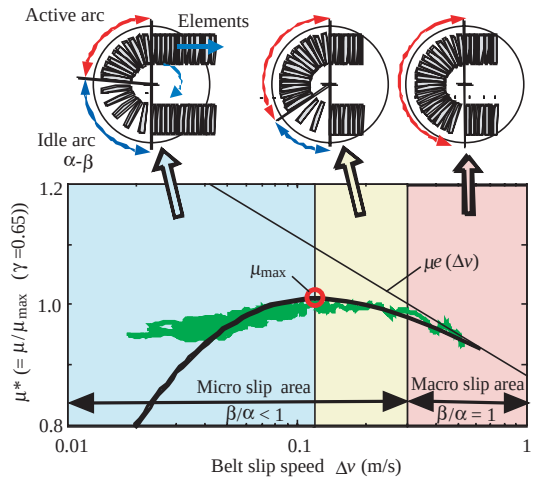

Fig. 12 State of power transmission.

Consequently, the element friction coefficient μe decreases, and the belt friction coefficient μ is saturated. In addition, in the slip speed region in which the maximum friction coefficient point has been exceeded, if the active arc ratio is less than 1, there are some elements that transmit no power. Therefore, it is thought that the region where the active arc ratio is less than 1 ($\beta/\alpha < 1$) is the micro slip region even though the belt slip speed is large. It is also thought that the belt endurance does not occur easily in this region.

In the region where the active arc ratio is equal to 1 ($\beta/\alpha = 1$), the belt μ–v characteristic corresponds to the element μ–v characteristic, and the belt friction coefficient μ decreases as the belt slip speed increases. In this region, all elements in the pulley slip uniformly. Therefore, this region is the macro slip region, and damage to the belt is a concern.

van Drogen[4] has researched the allowed belt slip limit, but the research examines only conditions in which the belt is not damaged in the all slip state. Therefore, the durability of the belt in the market is doubtful. On the other hand, it is thought that problems concerning durability of the belt do not occur easily if the belt slip is controlled so that the active arc ratio can become less than 1, placing the belt slip in the micro slip region.

4. Conclusion

In this paper, we proposed a belt friction expression model and obtained the following results:

(1) It was possible to forecast the change in the friction characteristic according to operating condition.

(2) The state of power transmission in the vicinity of the macro slip limit was clarified, and a new macro slip limit finding was obtained.

The CVT transmission efficiency of the high-speed cruise can be improved by use of these results to optimize the clamping force setting.[5]

References

1) Kluger, A. M. and Long, M. D. : "An Overview of Current Automatic, Manual and Continuously Variable Transmission Efficiencies and Their Projected Future Improvements", SAE Tech. Pap. Ser., No.1999-01-1259(1999)

2) Kobayashi, D., et al. : "A Study on the Torque Capacity of a Metal Pushing V-Belt for CVT's", SAE Tech. Pap. Ser., No.980822(1998)

3) Nishizawa, H., et al. : "Friction Characteristics Analysis for Clamping Force Setup in Metal V-Belt Type CVT", SAE Tech. Pap. Ser., No.2005-01-1462 (2005)

4) van Drogen, M., van der Laan, M. : " Determination of Variator Robustness Under Macro Slip Conditions for a Push Belt CVT", SAE Tech. Pap. Ser., No.2004-01-0480(2004)

5) Oshiumi, Y., et al. : "Optimal Control of the Clamping Force for Metal V-belt CVT", JSAE Tech. Pap., 20055108(2005)

(Report received on July 12, 2005)

Hiroyuki Nishizawa
Research fields : Transmission mechanism and control
Academic degree : Dr. Eng.
Academic society : Jpn. Soc. Mech. Eng., Soc. Autom. Eng. Jpn.
Award : JSME Young Eng. Award, 1996

Hiroyuki Yamaguchi
Research fields : Control and state estimation of power transmission system
Academic society : Jpn. Soc. Mech. Eng., Soc. Autom. Eng. Jpn.

Hideyuki Suzuki
Research fields : Power transmission system